Solar surface convection

By R. F. Stein †, Å. Nordlund ‡ J. F. Ripoll AND A. A. Wray

1. Introduction

The dynamics of the solar surface is driven by turbulent convection, magnetic fields and the escape of radiation. Convection transports energy upward through the outer third of the Sun and radiation carries it away to space. Convective motions transport angular momentum and produce differential rotation and the subsurface shear layer (Brummell *et al.* 1998;Miesch *et al.* 2000;Robinson & Chan 2001). Convection builds magnetic fields by dynamo action and transports it downward (Nordlund *et al.* 1992;Tobias *et al.* 1998; Cattaneo 1999;Tobias *et al.* 2001;Emonet & Cattaneo 2001). Magnetic flux tubes which emerge through the surface are shuffled around by the convective motions (Berger & Title 1996;Martinez Pillet *et al.* 1997;Berger *et al.* 1998; Lin & Rimmele 1999;Stolpe & Kneer 2000). This stresses the field whose subsequent relaxation heats the chromosphere and corona and controls their structure (Parker 1988;Galsgaard & Nordlund 1996;Judge *et al.* 1998). Convective motions generate the waves that produce the enhanced emission observed from the chromosphere (Carlsson & Stein 1997;Ulmschneider & Musielak 1998; Skartlien *et al.* 2000;Musielak & Ulmschneider 2001). Convection excites the p-mode oscillations and modifies their eigenfrequencies (Goldreich *et al.* 1994;Rosenthal *et al.* 1999;Stein & Nordlund 2001). Magnetic fields, oscillations and rotational shearing all alter convection itself (Hurlburt *et al.* 1996;Weiss *et al.* 1996; Brummell *et al.* 1998;Steiner *et al.* 1998;Tao *et al.* 1998). The interaction of these various processes controls the flux of radiation received by the Earth.

Convection is inherently three-dimensional, non-linear and non-local. As a result, most progress in understanding convection has come from analyzing numerical simulations. The computational challenge is to compute at high enough Reynolds number to include interactions of very disparate scales of motion. This requires simulations with very large 3D computational grids. We *cannot* hope to model the extremely large dynamic range and high Reynolds number that occur in the Sun. We *can* hope that our limited numerical capabilities will provide insight into what actually occurs in the Sun.

2. Large Scale and High Resolution Simulations

Recent observations with the Swedish 1-meter Solar Telescope have resolution of 70 km on the solar surface and the proposed Advanced Technology Solar Telescope will have a resolution of 30 km. With each new improvement in resolution new phenomena are discovered on the solar surface. The most recent has been the existence of striations in the bright side walls of granules observed toward the limb. To understand these high resolution observations, even higher resolution simulations of the solar surface convection are needed.

Local helioseismology can resolve structures as small as 30 Mm stable over 8 hour time

† Michigan State University
‡ NBIfAFG, University of Copenhagen, DK

intervals. The proper interpretation of such observations requires a simulated testbed on which the inversion techniques can be applied and compared with the actual properties. This requires simulating regions of 50 Mm width by 20 Mm depth to contain the observed short wavelength modes within the computational domain.

The horizontal velocity spectrum at the solar surface is a nearly featureless power law ($\propto$ wavenumber) with a peak at granular scales and a subsequent decline at still smaller scales. Yet the eye picks out "supergranulation" scale structures and there is controversy over their nature. Again this can be clarified by 50 Mm wide by 20 Mm deep simulations.

Such large scale simulations will also reveal the cause of the surface shear layer as well as provide insight into the emergence and dispersal of magnetic flux at the solar surface.

High resolution magneto-convection simulations have very small time steps because of the high Alfven speed in the upper photosphere and therefore require long simulations to mimic the behavior of the solar surface. Large scale simulations require a long time to relax the thermal structure at large depths and the dynamic structures at the large scales. To undertake both projects therefore requires an MHD code that can run efficiently on very many processors.

3. MHD Code

Our existing magneto-hydrodynamic code was modified to include a tabular equation of state and radiative transfer. Parallelization was implemented using Open MP with parallelization in as large blocks of code as possible, rather than individual loops. This avoids the overhead of repeated creation and destruction of multiple threads.

3.1. *Radiation*

Radiation from the solar surface produces the low entropy, high density fluid whose buoyancy work drives the convective motions. Observing the radiation from the solar surface provides us with our only information on what is occurring there. In the layer from which photons escape their mean free path is of order unity, so neither the diffusion approximation appropriate at large optical depths nor the optically thin approximation appropriate at very small optical depths is appropriate. To model radiative heating and cooling accurately requires solving the radiation transfer equation. A method is needed accurate enough to determine the radiative heating and cooling and efficient enough to calculate the 3D radiative transport for thousands of time steps on very large meshes. A balance between accuracy and speed is required. One project during the workshop was to test some of the approximations made in the convection simulation code in calculating the radiative transfer.

Radiative heating/cooling is the integral over wavelength of the difference between the opacity $\times$ the angle averaged intensity and the emission, or as it is usually written,

$$Q_{\rm rad} = 4\pi \int_\lambda \kappa_\lambda \left(J_\lambda - S_\lambda\right) d\lambda \ , \tag{3.1}$$

where κ_λ is the opacity or inverse of the photon mean free path, J_λ is the angle averaged intensity, and S_λ, the source function, is the ratio of the emissivity to the opacity. In the solar simulation code, to avoid roundoff errors from taking the difference between two comparable large numbers, we solve directly for the difference $J_\lambda - S_\lambda$ using the Feautrier method (Feautrier 1964). We assume Local Thermodynamic Equilibrium (LTE), so the source function is the Planck function. Two further approximating are made to greatly speed up the calculation. First, the number of wavelengths for which the transfer equation

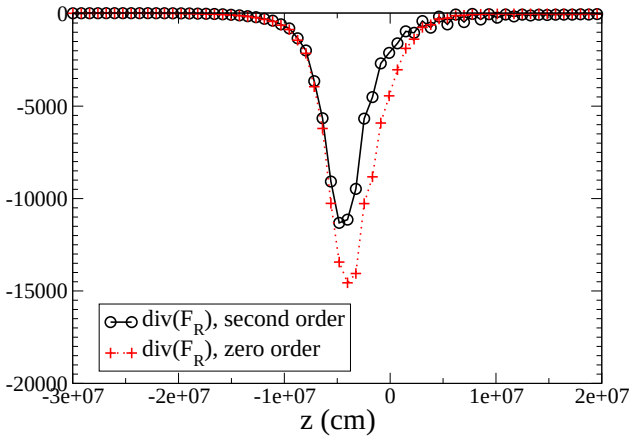

FIGURE 1. Divergence of the radiative flux for a 1D solar atmosphere comparing piecewise constant with second order Taylor expansion approximations for the source function and opacity.

is solved is drastically reduced by binning the opacity at each wavelength into four bins according to its magnitude and binning the source function the same way. Second, the transfer equation is solved along only 5 bi-directional rays – one vertical and four slanted rays through each point on the surface. (For details see Nordlund 1982; Stein & Nordlund 2003.)

Three issues were investigated: the spatial quadrature along a ray, the angular quadrature for the mean intensity, and alternate solution schemes used to solve for the radiation.

First consider the spatial quadrature along a ray. Fig 1 shows the radiative heating and cooling, for a one-dimensional mean solar atmosphere, calculated by the integral method, comparing a piecewise constant approximation with a second-order Taylor expansion for the opacity and source function. A piecewise constant approximation is inadequate unless a large number of depth points is used. In the solar code, both a piecewise linear approximation (trapezoidal rule) and a third order approximation for spatial integrals have been used. Accurate results further require an accurate calculation of the optical depth scale. With a third order integration scheme a spacing of 10 per decade in optical depth, or $\sim$ 15 km near optical depth unity, is needed. Note, in the solar photosphere, the source function is nearly linear in optical depth (Stein & Nordlund 1998, Fig 15).

Next, consider the angular quadrature needed to obtain the net heating/cooling or the mean intensity. Fig 2 shows the horizontally averaged radiative heating in a 3D snapshot from a solar convective simulation for 8 rays (2 polar and 4 azimuthal angles) and 48 rays (4 polar and 12 azimuthal angels) on the left. On the right is shown the horizontal rms of the radiative heating and the difference in the rms for 8 and 48 rays. The difference is less than 3%. Even though the optical depth surface has an rms variation of 35 km, so that hot and cold regions adjoin one another, most of the radiative cooling occurs vertically. However, when magnetic fields are present there is a larger variation ($\sim$ 300 km) in the optical depth unity surface and horizontal radiation transfer has a noticeable effect on the emergent intensity. However, even here the temperature at unit optical depth varies only slightly because of the high temperature sensitivity of the dominant

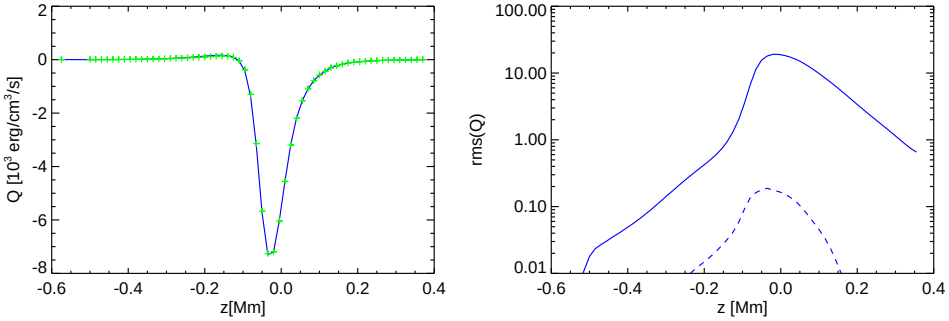

FIGURE 2. Radiative cooling. Left: average heating/cooling for 8 and 48 rays. Right: rms heating/cooling for 48 rays (solid) and difference between 8 and 48 rays (dashed).

opacity source (H^- ions). In the solar simulation code, one vertical and one non-vertical angle with 4 azimuthal angles are used, which provides approximately 1reason such few angles provides sufficient accuracy in the solar photosphere (more rays are needed in the chromosphere) is the small temperature variation at unit optical depth from which the radiation emerges (see Stein & Nordlund 1998 Fig. 22).

The vertical extent of the photosphere (500 km) is small compared to the radius of the Sun, which therefore appears as an infinite planar source. The radiative anisotropy, is nearly zero below the surface, increases through the photosphere, reaching a maximum of ~ 0.6 at the transition to the chromosphere. Farther away the anisotropy is larger, approaching one as the Sun recedes to a point source.

An alternative method of calculating the radiation is the moment model, in which four conservation equations for the radiation energy density and the three components of the radiative flux vector are solved at every point in the computational domain (Mihalas & Mihalas 1984). To use such a method, the system of moment equations must be closed by relating the radiation stress tensor to the radiation energy density and flux. This is done by means of so called "Eddington factors", which express the degree of anisotropy and act as a flux limiter(Levermore 1984). If the Eddington factor could be accurately determined analytically, this would be a useful method to obtain the radiative heating/cooling without the necessity of solving the radiative transfer equations. The radiative heating/cooling from several moment models, applied to a one-dimensional, horizontally averaged, solar atmosphere is shown in Fig. 3 (left). Two flux-limited moment models, derived using the maximum entropy closure (Minerbo 1979) the M_1 model (Levermore 1984;Fort 1997)† and the M_1^+ model (Ripoll & Wray 2004), are compared to integral RTE solvers. Both models are computed with the second order scheme used in Ripoll *et al.* (2002). They rather accurately capture the cooling near optical depth unity. However, both moment methods overestimate absorption in the atmosphere, for unknown reasons. Equilibrium is approached for $z > 0$ ‡.

The anisotropy and the Eddington closure factor are shown in Fig. 3 (right). It can

† see Ripoll (2004) for more references concerning this model, and, Jensen et al. in this volume.

‡ The source term of both moment models has been truncated to zero when the difference between the temperature and the radiative temperature is less then $1K$. This is done in order to avoid numerical wiggles which are generated by the subtraction of two large numbers, the emission and absorption terms, which should almost cancel to give equilibrium.

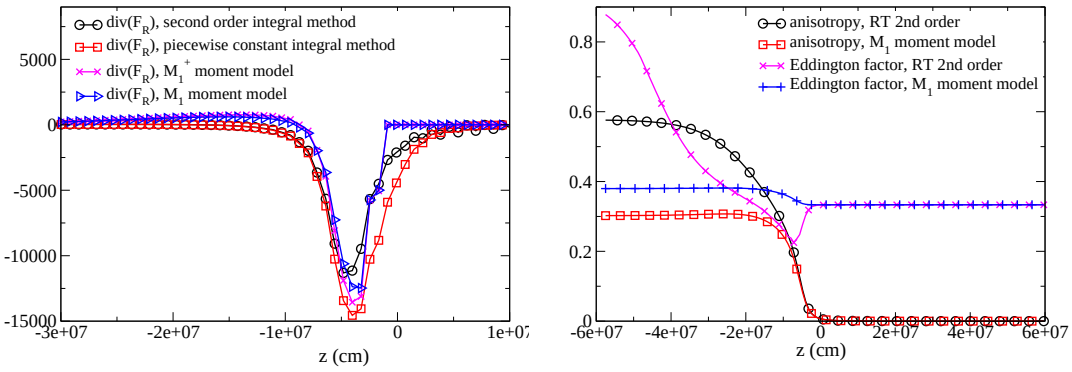

FIGURE 3. Left: radiative cooling computed with 4 different methods. Right: anisotropy and Eddington factor computed by the M_1 model and a RTE solver.

be seen that the anisotropy is below 0.6 ¶, and that the moment methods underestimate this value in the atmosphere. The Eddington factor found by the RTE solver is below 1/3 near the surface, which cannot be reproduced by any existing moment model (for which the lower bound is 1/3, the equilibrium value). The M_1^+ model is only flux-limited for anisotropies larger than 1/2 (to avoid non-physical results and to guarantee numerical stability) and is otherwise equivalent to P_1 ‖. Since $f < 1/2$ everywhere for this particular solar profile, the M_1^+ Eddington factor is simply 1/3 (like P_1), but this may not hold for all solar profiles. It should be noted that the anisotropy is always lower for one-dimensional atmospheres than for three-dimensional ones. In an evolving three-dimensional configuration, different hydrodynamic states may produce larger anisotropies and the flux will need to be limited. The fact that the anisotropy and the Eddington factor from the moment models are not equivalent to the RTE values on the whole domain yet the average radiative cooling/heating is similar, leads to the conclusions that, first, only a small transition region around the surface matters for the escape of radiation, and second, that radiation is primarily determined by its emission and absorption rather than by its direction of propagation, for our one-dimensional atmosphere.

4. High Resolution, Small Scale Simulations

We have simulated a small patch near the surface of the Sun with horizontal size 6 × 6 Mm and a height range from the temperature minimum at 0.5 Mm above - down to 2.5 Mm below - the visible surface, on a grid of 253 × 253 × 163 zones. Initially we imposed a uniform vertical magnetic field of 250 G on a snapshot of well established hydrodynamic solar convection. The magnetic field is rapidly swept by the granular and mesogranular flows into the mesogranular scale downflow lanes and concentrated to kiloGauss strength.

We have used these simulation results to synthesize center-to-limb G-band images (Fig. 4). Towards the limb the simulations show "hilly" granulation with dark bands on the far side, bright granulation walls and striated faculae, similar to observations. At disk center G-band bright points are flanked by dark lanes. The increased brightness in

¶ for 1D configurations, the upper limit of f is around 1
‖ The P_1 closure assumes isotropic propagation and has no flux limiter.

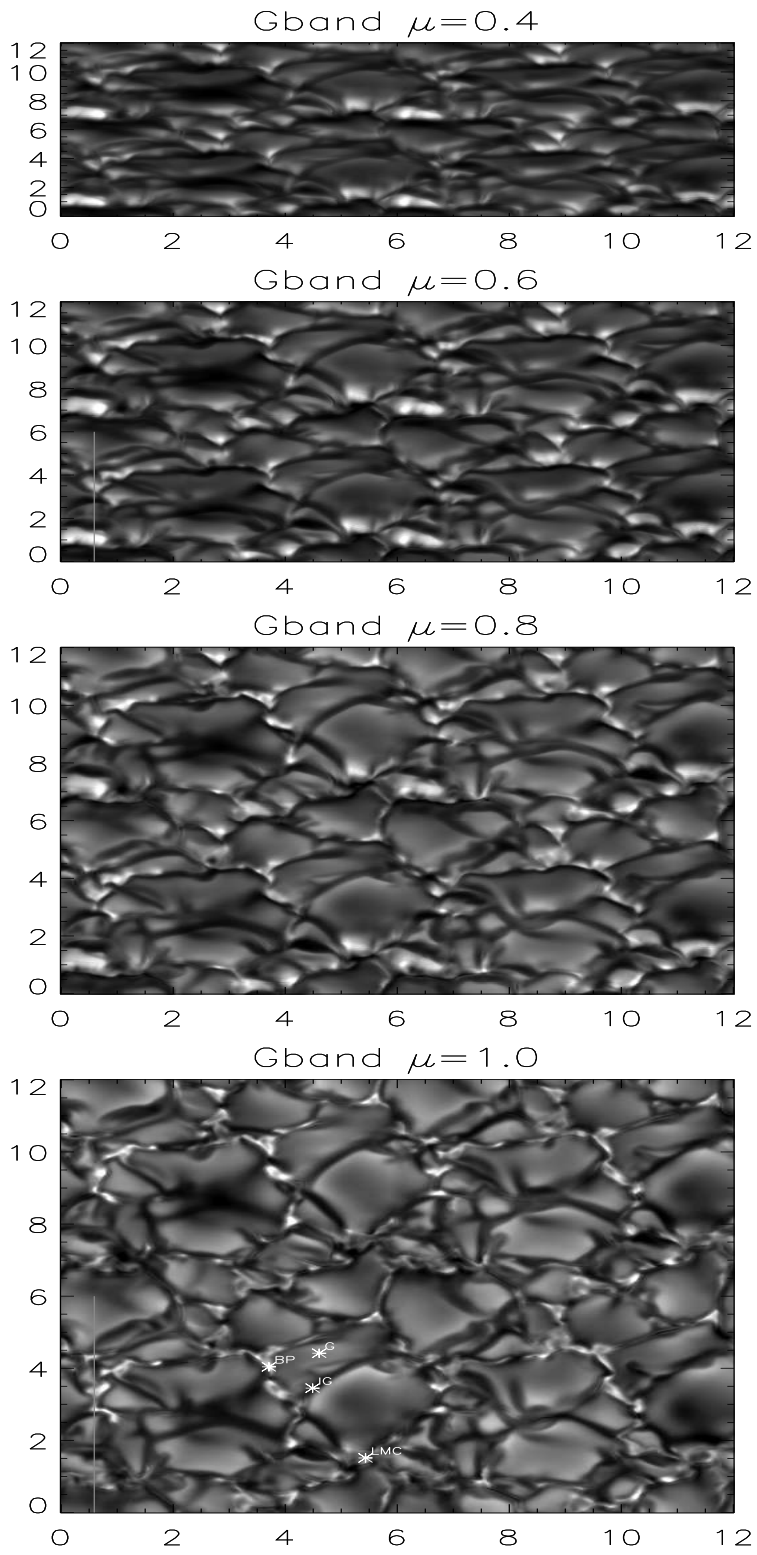

FIGURE 4. G-band images synthesized from magneto-convection simulation. Four images at 30 sec intervals have been combined (UL,LL,UR,LR) to make the patterns more obvious.

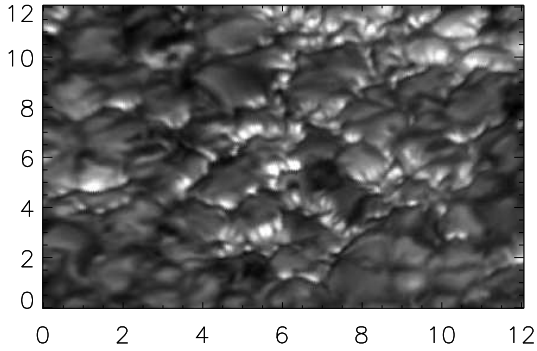

FIGURE 5. Observed G-band intensity at $\mu = 0.63$, from the Swedish 1-m Solar Telescope (June 2003). Data reduction using Multi-Frame-Blind-Deconvolution performed by Luc Rouppe van der Voort. Note "hilly" granulation with dark bands on the far side, bright granulation walls and striated faculae.

magnetic elements is due to their lower density compared with the surrounding intergranular medium. One thus sees deeper layers where the temperature is higher. At a given geometric height, the magnetic elements are cooler than the surrounding medium. In the G-band, the contrast is further increased by the destruction of CH in the low density magnetic elements. The optical depth unity surface is very corrugated. Bright granules have their continuum optical depth unity 80 km above the mean surface, the magnetic elements 200-300 km below. The horizontal temperature gradient is especially large next to flux concentrations. When viewed at an angle, the deep magnetic elements' optical surface is hidden by the granules and the bright points are no longer visible, except where the "magnetic valleys" are aligned with the line of sight. Towards the limb, the low density in the strong magnetic elements causes unit line-of-sight optical depth to occur deeper in the granule walls behind, than for rays not going through magnetic elements, and variations in the field strength produce a striated appearance in the bright granule walls (Carlsson *et al.* 2004). An observed G-band image is shown is Fig. 5.

We would now like to perform similar simulations at still higher resolution because we believe that magnetic instabilities will show up at small scales and contribute to the striated appearance of the granule walls, and because the ATS Telescope will provide images of higher resolution than reliably obtainable from our current 25 km horizontal grid size simulations.

5. Large Scale Simulations

Large scale simulations require a long time to develop the large scale dynamical structures because the ratio of velocity to size is small. Large scale simulations require a long time to relax the thermal structure at large depths because the ratio of energy flux to energy density is small. As a first step, we have begun a simulation of 24 Mm $\times$ 24 Mm horizontal size and 9 Mm depth. A time span comparable to a few turnover times of the largest flows in the computational domain is required. This run was started from a 12 Mm wide simulation doubled in each of the periodic horizontal directions with a small perturbation added to break the symmetry (Fig. 6). This relaxation is proceeding. We expect it to develop structure on the computational box (24 Mm). When this domain is relaxed, it will be doubled in size both horizontally and vertically, to reach 48 Mm $\times$ 18 Mm deep.

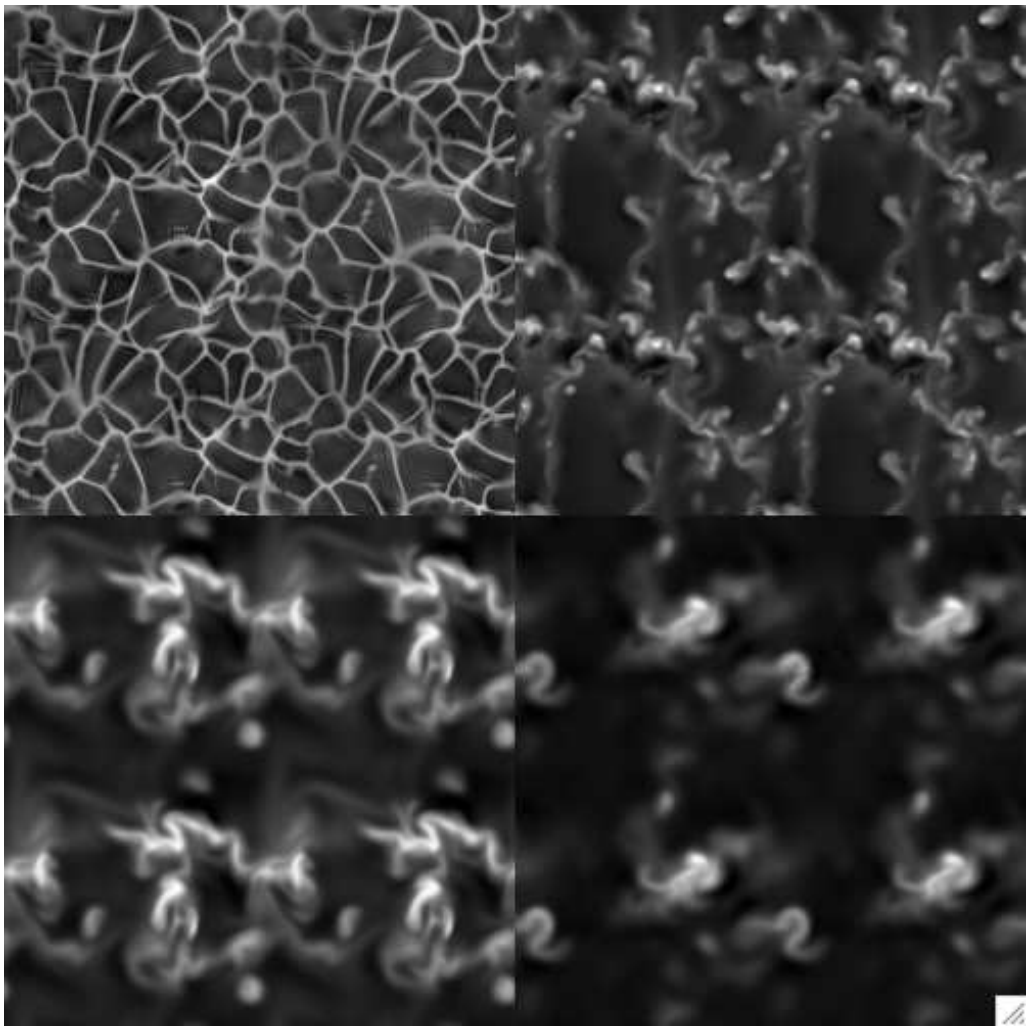

FIGURE 6. Vertical velocity at the surface (UL), 3 Mm (UR), 6 Mm (LL) and 9 Mm (LR) depth. It is clear that the initial structures still need to evolve and larger scale structures need time to develop.

6. Convection Spectrum

The spectrum of solar convection is not separable into spatial and temporal components because the temporal spectrum varies with the spatial wave number. It can be best fit by an analytic expression of the form

$$P_V(\omega, k) = a/(\omega^2 + w^2)^{p(k)}$$

Both the exponent, p, and width, w, increase with increasing spatial wave number (Fig. 7). In the past analytic studies have assumed that the turbulent convective energy spectrum is separable into independent spatial and temporal factors. The more complicated actual situation may explain some of the difficulties that these overly simplified models experience.

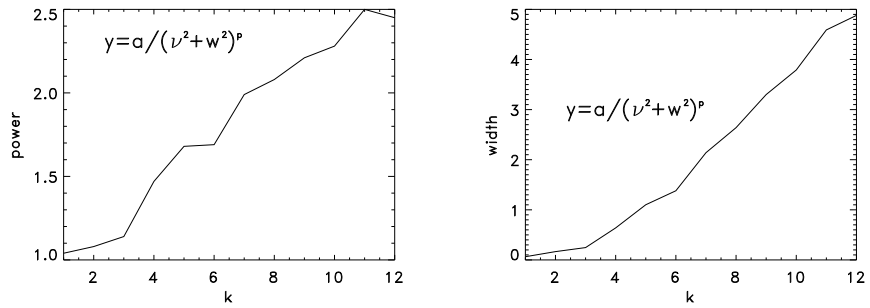

FIGURE 7. Analytic fit to temporal spectrum of vertical velocity in a high resolution convection simulation. Both the exponent of the power law and the width of the low frequency plateau increase with increasing spatial wave number.

REFERENCES

BERGER, T. E., LOEFDAHL, M. G., SHINE, R. S., AND TITLE, A. M. 1998 Measurements of solar magnetic element motion from high-resolution filtergrams. *ApJ* **495**, 973.

BERGER, T. E. AND TITLE, A. M. 1996 On the dynamics of small-scale solar magnetic elements. *ApJ* **463**, 365.

BRUMMELL, N. H., HURLBURT, N. E., AND TOOMRE, J. 1998 Turbulent compressible convection with rotation. II. mean flows and differential rotation. *ApJ* **493**, 955.

CARLSSON, M. AND STEIN, R. F. 1997 Formation of solar calcium H and K bright grains. *ApJ* **481**, 500.

CARLSSON, M., STEIN, R. F., NORDLUND, Å., SCHARMER, G.B. 2004 Observational manifestations of solar magneto-convection — center-to-limb variation. *ApJ* **610**, L137.

CATTANEO, F. 1999 On the origin of magnetic fields in the quiet photosphere. *ApJ* **515**, L39–L42.

EMONET, T. AND CATTANEO, F. 2001 Small-scale photospheric fields: observational evidence and numerical simulations., *ApJ* **560**, L197–L200.

FEAUTRIER, P 1964 Sur la resolution numerique de l'equation de transfert. *Comptes Rendus Academie des Sciences Paris* **258**, 3189.

FORT, J. 1997 Information-theoretical approach to radiative transfer., *Phys. A.*, **243**, 275-303.

GALSGAARD, K. AND NORDLUND, Å. 1996 The heating and activity of the solar corona: I. Boundary shearing of an initially homogeneous magnetic field. *Journal of Geophysical Research* **101(A6)**, 13445–13460.

GOLDREICH, P., MURRAY, N., AND KUMAR, P. 1994 Excitation of solar p-modes. *ApJ* **424**, 466–479.

HURLBURT, N. E., MATTHEWS, P. C., AND PROCTOR, M. R. E. 1996 Nonlinear compressible convection in oblique magnetic fields. *ApJ* **457**, 933.

JUDGE, P. G., HANSTEEN, V., WIKSTOL, O., WILHELM, K., SCHUEHLE, U., AND MORAN, T. 1998 Evidence in support of the "nanoflare" picture of coronal heating from SUMER data. *ApJ* **502**, 981.

LEVERMORE, D. 1984 Relating Eddington factors to flux limiters., *Jour. Quant. Spectrosc. Radiat. Transfer*, **32(2)**, 149-160.

LIN, H. AND RIMMELE, T. 1999 The granular magnetic fields of the quiet Sun. *ApJ* **514**, 448–455.

MARTINEZ PILLET, V., LITES, B. W., AND SKUMANICH, A. 1997 Active region magnetic fields. I. plage fields. *ApJ* **474**, 810.

MIESCH, M. S., ELLIOTT, J. R., TOOMRE, J., CLUNE, T. L., GLATZMAIER, G. A., AND GILMAN, P. A. 2000 Three-dimensional spherical simulations of solar convection. I. differential rotation and pattern evolution achieved with laminar and turbulent states. *ApJ* **532**, 593–615.

MIHALAS, D. AND MIHALAS, B.W . 1984 Foundation of radiation hydrodynamics. *Oxford University Press*.

MINERBO, D. 1984 Maximum entropy Eddington factors, *Jour. Quant. Spectrosc. Radiat. Transfer*, **20**, 541-545.

MUSIELAK, Z. E. AND ULMSCHNEIDER, P. 2001 Excitation of transverse magnetic tube waves in stellar convection zones. I. Analytical approach. *Astron. Astrophys.* **370**, 541–554.

NORDLUND, Å. 1982 Numerical simulations of the solar granulation. I - basic equations and methods. *Astron. Astrophys.* **107**, 1–10.

NORDLUND, Å., BRANDENBURG, A., JENNINGS, R. L., RIEUTORD, M., ROUKOLAINEN, J., STEIN, R. F., AND TUOMINEN, I. 1992 Dynamo action in stratified convection with overshoot. *ApJ* **392**, 647–652.

PARKER, E. N. 1988 Nanoflares and the solar x-ray corona. *ApJ* **330**, 474–479.

RIPOLL, J.-F. 2004 An average formulation of the M_1 radiation model with mean absorption coefficients and presumed probability functions for turbulent flows., *Jour. of Quant. Spectrosc. & Radiat. Transfer.*, **83**, 493-517.

RIPOLL, J.-F., WRAY, A.,A. 2004 A half-moment model for radiative transfer in a 3D gray medium and its reduction to a moment model for hot, opaque sources., *Jour. Quant. Spectrosc. Radiat. Transfer*, in press.

RIPOLL, J.-F., DUBROCA, B., AUDIT, E. 2002 A factored operator method for solving coupled radiation-hydrodynamics models., *Trans. Theory and Stat. Phys.*, **31**(4-6), 531-557.

ROBINSON, F. J. AND CHAN, K. L. 2001 A large-eddy simulation of turbulent compressible convection: differential rotation in the solar convection zone., *MNRAS* **321**, 723–732.

ROSENTHAL, C. S., CHRISTENSEN-DALSGAARD, J., NORDLUND, A., STEIN, R. F., AND TRAMPEDACH, R. 1999 Convective contributions to the frequencies of solar oscillations. *A&A* **351**, 689–700.

SKARTLIEN, R., STEIN, R. F., AND NORDLUND, Å. 2000 Excitation of chromospheric wave transients by collapsing granules. *ApJ* **541**, 468–488.

STEIN, R. F. AND NORDLUND, Å. 1998 Simulations of solar granulation: I. General properties. *ApJ* **499**, 914-933.

STEIN, R. F. AND NORDLUND, Å. 2001 Solar oscillations and convection. II. excitation of radial oscillations. *ApJ* **546**, 585–603.

STEIN, R. F. AND NORDLUND, Å. 2003 Radiation transfer in 3D numerical simulations. *Stellar Atmosphere Modeling*, eds. I. Hubeny, D. Mihalas, K. Werner, ASP Conf. Ser. **288**, 519–532.

STEINER, O., GROSSMANN-DOERTH, U., KNOELKER, M., AND SCHUESSLER, M. 1998 Dynamical interaction of solar magnetic elements and granular convection: results of a numerical simulation. *ApJ* **495**, 468.

STOLPE, F. AND KNEER, F. 2000 On weak magnetic flux structure of the Sun. *Astron. & Astrophys.* **353**, 1094.

TAO, L., WEISS, N. O., BROWNJOHN, D. P., AND PROCTOR, M. R. E. 1998 Flux separation in stellar magnetoconvection. *ApJ* **496**, L39.

TOBIAS, S. M., BRUMMELL, N. H., CLUNE, T. L., AND TOOMRE, J. 1998 Pumping of magnetic fields by turbulent penetrative convection. *ApJ* **502**, L177.

TOBIAS, S. M., BRUMMELL, N. H., CLUNE, T. L., AND TOOMRE, J. 2001 Transport and storage of magnetic field by overshooting turbulent compressible convection. *ApJ* **549**, 1183–1203.

ULMSCHNEIDER, P. AND MUSIELAK, Z. E. 1998 On the generation of nonlinear magnetic tube waves in the solar atmosphere. II. Longitudinal tube waves., *Astron. Astrophys.* **338**, 311–321.

WEISS, N. O., BROWNJOHN, D. P., MATTHEWS, P. C., AND PROCTOR, M. R. E. 1996 Photospheric convection in strong magnetic fields *MNRAS* **283**, 1153–1164.